



Influence of Sintering Temperatures on Structure and Electrical Conductivity of TiO₂ Cathode

ZEQUAN LI^{1,2,*}, NA ZHANG¹, CHENGUANG BAI², DONGMEI JIAN¹, LIYUE RU¹ and HAIHUA WANG¹

¹College of Chemistry and Chemical Engineering, Chongqing University, Chongqing 400044, P.R. China

²College of Materials Science and Engineering, Chongqing University, Chongqing 400044, P.R. China

*Corresponding author: Tel: +86 23 65432347; E-mail: lzq0313@cqu.edu.cn

(Received: 16 November 2010;

Accepted: 20 July 2011)

AJC-10183

The influence of sintering temperatures on the structure and electrical property of TiO₂ cathode was investigated with regards to the crystal structure and composition, microstructure, oxygen vacancies, surface properties and electrical conductivity. The as-products were characterized by powder X-ray diffraction (XRD), X-ray photoelectron spectroscopy (XPS), scanning electron microscopy (SEM), digital four-point probe conductivity instrument (DFFPCI) and accelerated surface area and porosimetry system (ASAP). XRD analysis confirms that anatase phase TiO₂ at 700 °C transformed to rutile phase TiO₂ and TiO_{1.95} with the increase of sintering temperatures to 850 °C and 950 °C. The Ti^{2p} binding energy of TiO₂, as studied by XPS, is discussed in terms of the valence state of the titanium ions. Digital four-point probe conductivity instrument analysis indicate that the electrical conductivity increase with the rise of temperature. Scanning electron microscopy and accelerated surface area and porosimetry system analysis indicate that the grain of the obtained TiO₂ increase but nitrogen storage properties decrease with the increase of sintering temperatures. Moreover, the experimental results show that the electrical conductivity of TiO₂ increases with the rise of the temperature.

Key Words: TiO₂, Cathode, Sintering temperature, Surface, Microstructure.

INTRODUCTION

Over the past decade, TiO₂ has attracted much attention due to its favourable physical, optical and electrical properties and various potential applications in various fields such as gas sensor^{1,2}, thin film capacitors^{3,4}, photocatalyst^{5,6} and solar cells^{7,8}, etc. As is known to all, TiO₂ is an oxygen-deficient compound, temperature and oxygen partial pressure can greatly affect its crystal structure, chemical composition and properties. TiO₂ has three phases of brookite, anatase and rutile at different temperatures and the metastable phase anatase differs in electronic properties from the phase rutile. Moreover, rutile structure is thermodynamically more stable than the anatase structure and also is more dense. On the other hand, pure TiO₂ is electrically insulating or poorly conductive and its electrical conductivity is small ($< 10^{-13}$ S/cm). In general, sintering is a key step in the preparation of TiO₂ cathode and sintering temperature has a large effect on the phase, structure and electronic transport properties of the final products.

In recent years, many efforts have been devoted to investigate the formation of non-stoichiometric TiO₂ and various doping TiO₂ and its electronic properties, photoelectrochemical properties and wettability. For instance, Abdel-Aziz *et al.*⁹ studied the dependence of the electrical conductivity in the temperature range (148-373 K) of polycrystalline TiO₂ and

Ti₂O₃. Yakuphanoglu *et al.*¹⁰ investigated the electrical, microstructure and crystal structure properties of Ni-doped TiO₂. Wang *et al.*¹¹ studied the nonlinear electrical behaviour and dielectric properties of (Ca, Ta)-doped TiO₂ ceramics which were obtained by sintering at 1300 °C. Meng Fan-ming investigated influence of sintering temperature on nonlinear electrical properties of (Sr, Bi, Si, Ta)-doped TiO₂-based varistor ceramics which were obtained by sintering at 1350 °C¹². However, little attention has been paid to the detailed effects of the sintering temperatures on the microstructure, surface properties and electrical conductivity of TiO₂ cathode.

In this paper, we investigate the influence of sintering temperatures on the phase, microstructure, surface properties, oxygen vacancies and electrical conductivity properties of TiO₂ cathode. The chemical compositions of the as-prepared TiO₂ cathode sintered at different temperatures are measured by XRD and XPS. The porosity and mean pore size of TiO₂ cathode at different temperatures are also investigated. Moreover, the effect of sintering temperature on the electrical conductivity properties of TiO₂ cathode are also investigated.

EXPERIMENTAL

Synthesis of TiO₂ cathode: TiO₂ (AP, 99.9 %) powders were sintered at a rate of 10 °C/min in the tubular resistance furnace (SGM6816BK) under argon atmosphere for 5 h. After

that, they were cooled to room temperature. Then they were pressed by 16 MPa and sintered at different temperatures to make into 0.5 g TiO₂ pellets. The sintering temperatures were 700, 850 and 950 °C respectively. The TiO₂ pellets sintered at different temperatures were assembled into the cathode. Finally, TiO₂ cathode were obtained.

Characterization: The phase composition, the surface topography and chemical analysis of TiO₂ sintered were performed by XRD-6000 X-ray diffraction (XRD) with CuK_α radiation ($\lambda = 0.15406$ nm) through a continuous scan mode with speed of 4 °/min, VEGA ILMU scanning electron microscope (SEM) and X-sight energy dispersive spectrum (EDS). The oxygen vacancies of samples sintered were characterized by ESCALAB250 X-ray photoelectron spectra (XPS) with AlK_α ($h\nu = 1486.6$ eV) as an excitation source. The XPS peak positions of each element were corrected by using of C1s (285.0 eV). The electrical conductivity of TiO₂ pellets were performed with a digital four-point probe conductivity instrument (DFPPCI; SX1934). The surface properties and pore-size distribution were determined by ASAP 2010 (accelerated surface area and porosimetry system).

RESULTS AND DISCUSSION

Effect of sintering temperatures on phase composition of TiO₂ cathode: Fig. 1 shows the XRD patterns of as-prepared TiO₂ pellets sintered for the same reaction time of 5 h at (a) 700 °C, (b) 850 °C and (c) 950 °C, respectively. The crystalline phase of the pellets sintered at 700 °C was dominantly anatase in Fig. 1(a), whereas the pellets treated at 850 and 950 °C show peaks characteristic of both the rutile TiO₂ and rutile TiO_{1.95} phase in Fig. 1(b) and Fig. 1(c). With increasing of sintering temperature, the intensities of the peaks increased to some extent. The crystal size of the prepared TiO₂ sintered at 700, 850 and 950 °C were estimated to be 65.3, 92.0 and 103.0 nm in diameter by the Scherrer's equation, respectively. The biphase TiO₂ sintered at 850 °C contains about 50 % of the rutile TiO_{1.95} phase, while the biphase TiO₂ sintered at 950 °C contains about 59 % of the rutile TiO_{1.95} phase. The phase composition of the samples can be calculated from the equation¹³:

$$X_R = 1 - \left[1 + 1.26 \left(\frac{I_R}{I_A} \right) \right]^{-1}$$

where X_R is the weight fraction of rutile TiO_{1.95} in the mixture, I_R and I_A are the peak intensities of the rutile TiO_{1.95} and rutile TiO₂ diffractions, respectively.

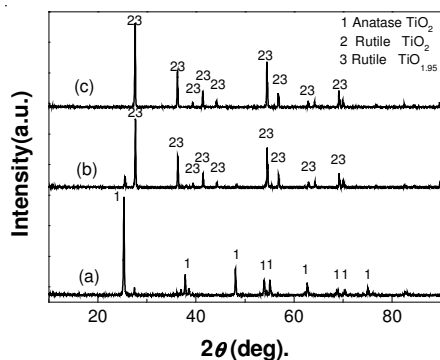
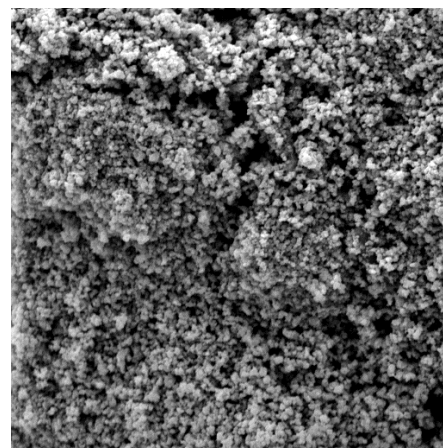


Fig. 1. XRD patterns of as-prepared TiO₂ cathode sintered for the same reaction time of 5 h at (a) 700 °C (b) 850 °C and (c) 950 °C

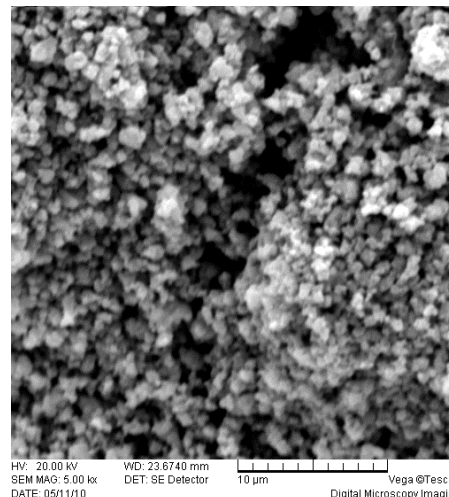
Effect of sintering temperatures on morphologies of TiO₂ cathode: The scanning electron micrographs (SEM) of TiO₂ pellets sintered at different temperatures for 5 h are presented in Fig. 2. It is seen in figures that with the increase of temperature, the TiO₂ grains are growing larger and tending to be homogenized, while the porosity decreases and monolithic structure tends to be more densification. The grains in microstructure may have an important effect on electronic properties of the samples. EDX of TiO₂ pellets sintered for the same reaction time of 5 h at (a) 700 °C, (b) 850 °C and (c) 950 °C, respectively is shown in Fig. 3 and the corresponding contents of elements are given in Table-1, which indicate that the samples have polycrystalline and the sample includes three elements (Ti, O and Au). Gold is introduced in process of the sample prepared for SEM inspection. The results show that content of titanium increases and oxygen decreases with the rise of temperature.

TABLE-1
THE CONTENTS OF ELEMENTS FOR SAMPLES
SINTERED AT DIFFERENT TEMPERATURES

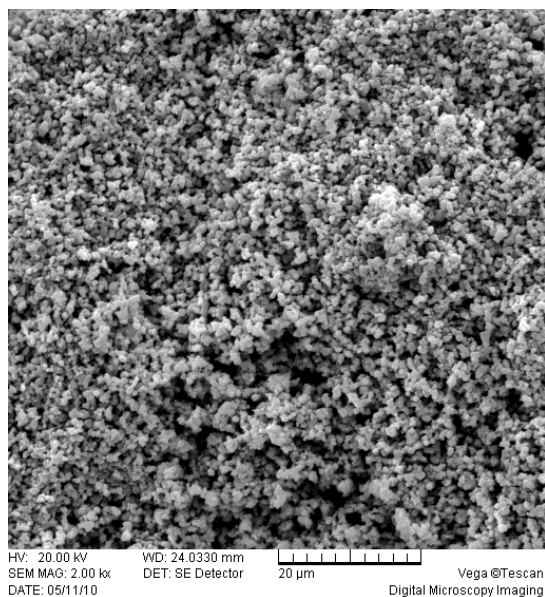
Temp. (°C)	Content of elements (wt %)		
	Ti	O	Au
700	50.91	35.20	13.89
850	54.86	32.33	12.81
950	60.09	27.19	12.72



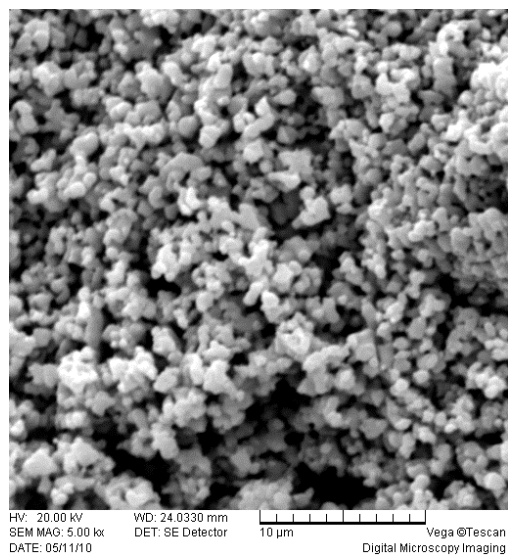
a₁



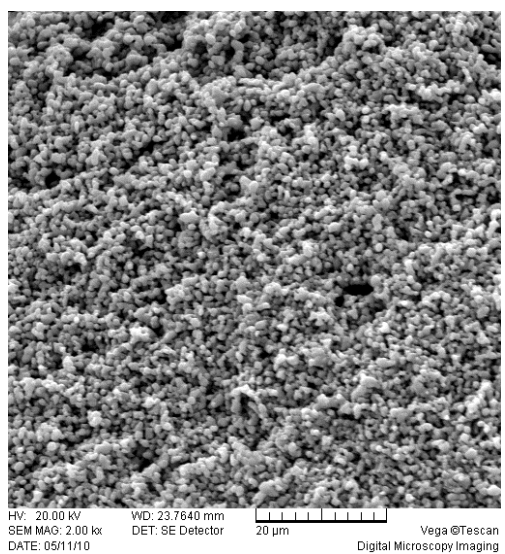
a₂



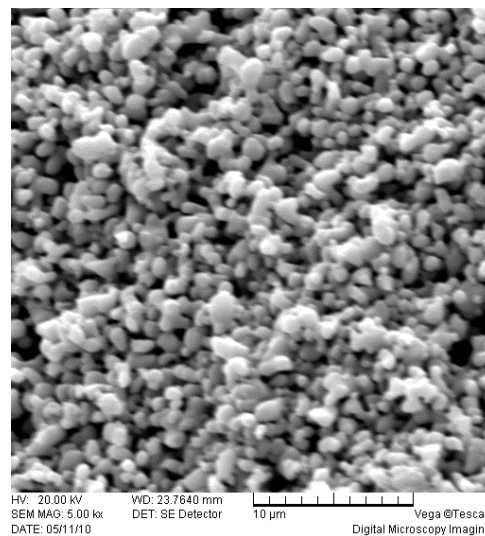
b₁



b₂



c₁



c₂

Fig. 2. SEM morphologies of TiO₂ cathode sintered for the same reaction time of 5 h at (a) 700 °C (b) 850 °C and (c) 950 °C

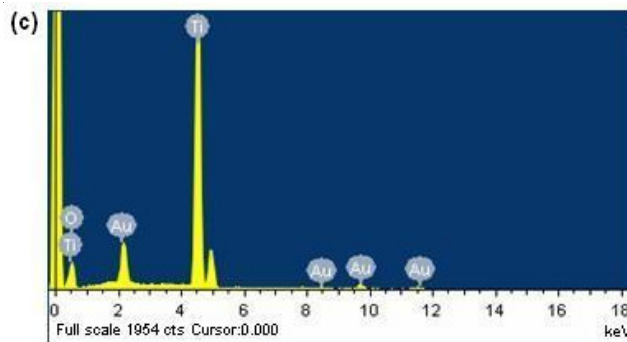
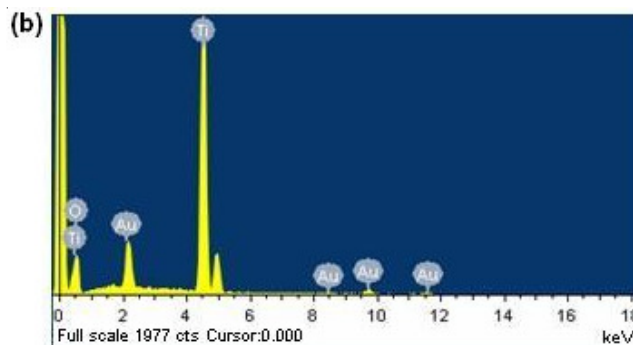
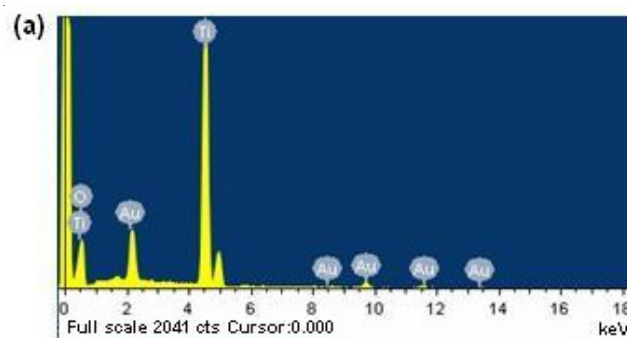


Fig. 3. EDX photographs and chemical composition of TiO₂ cathode sintered for the same reaction time of 5 h at (a) 700 °C (b) 850 °C and (c) 950 °C

Effect of sintering temperatures on the surface areas and pore-size distribution: The surface parameters of surface area and the data calculated from the t -plot were estimated by the low-temperature nitrogen adsorption at relative pressures (P/P_0) in the range of 0.0-1.0. The BET surface areas of TiO₂ cathode sintered at 700, 850 and 950 °C are 4.9327, 2.4437 and 1.6419 m²/g, respectively. With the increase of temperature, the specific surface areas of TiO₂ cathode decrease.

The textural parameters of TiO₂ cathode were obtained by nitrogen adsorption-desorption experiment at 77 K. Fig. 4 shows the nitrogen adsorption-desorption isotherms and the corresponding pore size distributions of the TiO₂ cathode sintered at different temperatures. As shown in Fig. 4(a₁), (b₁), (c₁), the similar nitrogen adsorption-desorption isotherms of all samples can be classified as a type IV isotherm, each hysteresis loop is type H₂ and a steep increase in nitrogen volume adsorbed at higher P/P_0 (by the mechanism of capillary condensation) indicate a typical of a mesoporous material¹⁴⁻¹⁷. Furthermore, the pore size distributions are reported in Fig. 4(a₂), (b₂), (c₂) for TiO₂ sintered at various temperatures and concentrate below 50 nm. According to IUPAC classification, pores within porous materials can be divided into micropore (width less than 2 nm), mesopore (width between 2 and 50 nm) and macropore (width greater than 50 nm)¹⁸⁻²⁰. From above analysis, we can obtain that the samples sintered at 700, 850 and 950 °C are mesoporous structure.

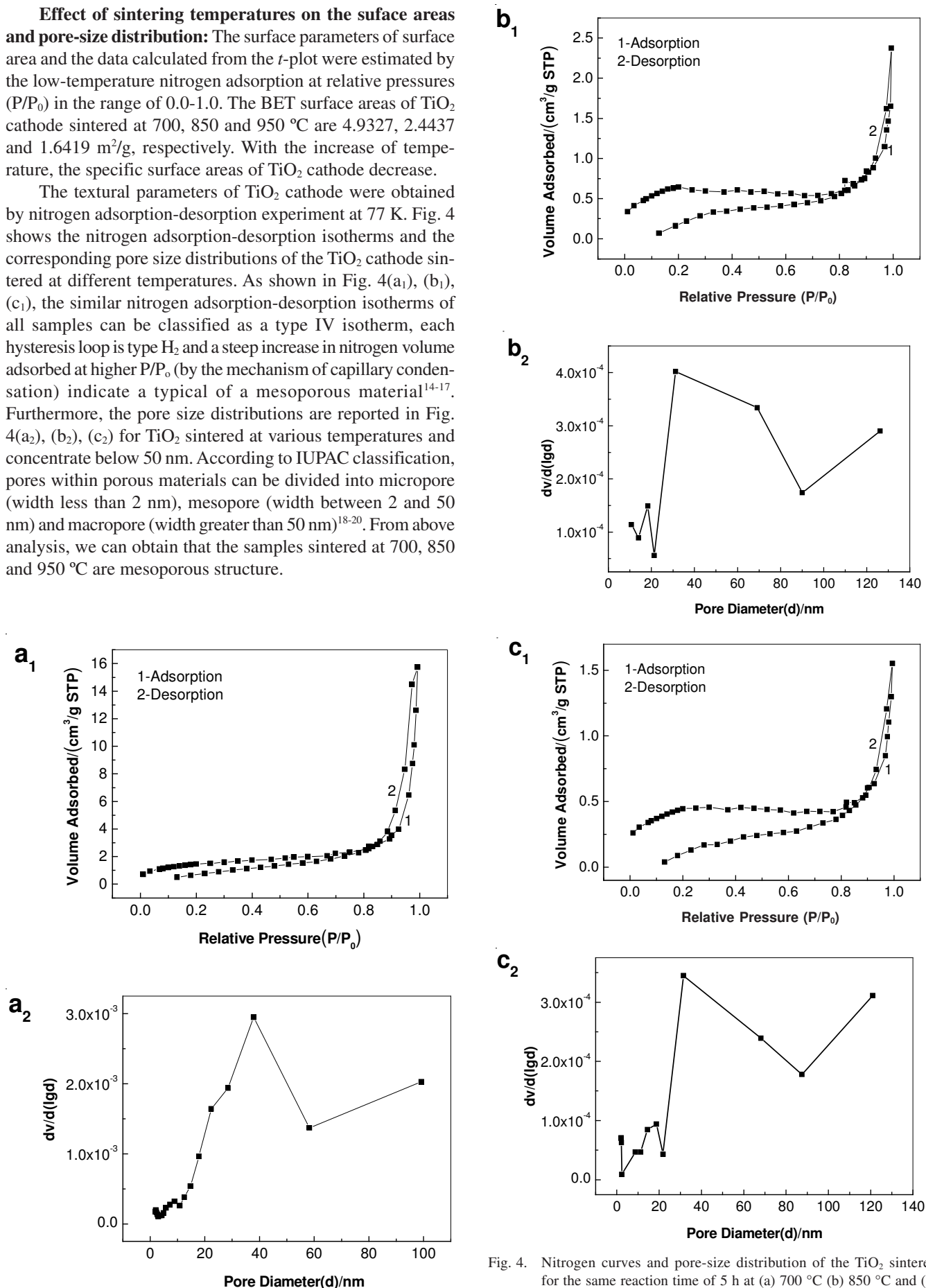


Fig. 4. Nitrogen curves and pore-size distribution of the TiO₂ sintered for the same reaction time of 5 h at (a) 700 °C (b) 850 °C and (c) 950 °C

Effect of sintering temperatures on the electrical conductivity of TiO₂ cathode: In general, electrical conductivity of TiO₂ can be enhanced by doping. For instance, da Silva *et al.*²¹ studied the electrical conductivity of TiO₂ single crystals doping of chromium ions implanted with 140 keV at room temperature. It changed from variable to fixed range hopping. Patil *et al.*²² investigated the electrical resistivity of TiO₂ doped WO₃ thin films. It decreased with the increase of temperature. Karthik *et al.*²³ reported nickel-doped anatase TiO₂ nanoparticles by sol-gel method, the conductivity of which decreases with increasing Ni-dopant concentration. Holt *et al.*²⁴ demonstrated the electrical conductivity of Cr₂O₃ doped with TiO₂. It decreased with TiO₂ concentration higher than 10 mol %. However, not only doping but also sintering can be changed the electrical conductivity of TiO₂ cathode. In present investigation, the electrical conductivity of the as-prepared TiO₂ pellets is shown in Fig. 5. With the increase of temperature from 700-950 °C, the electrical conductivity of the TiO₂ pellets slightly increased, indicating the semiconductor behaviour of TiO₂ cathode. The electrical conductivity of the samples may be analyzed by the well-known Arrhenius relation¹⁰:

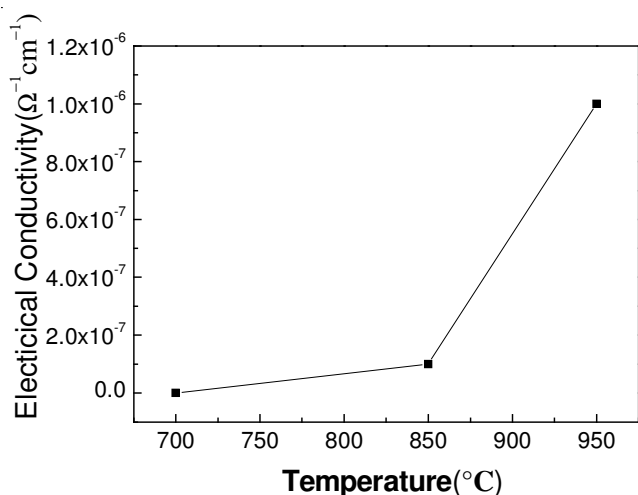


Fig. 5. Electrical conductivity of TiO₂ cathodes sintered at different temperatures

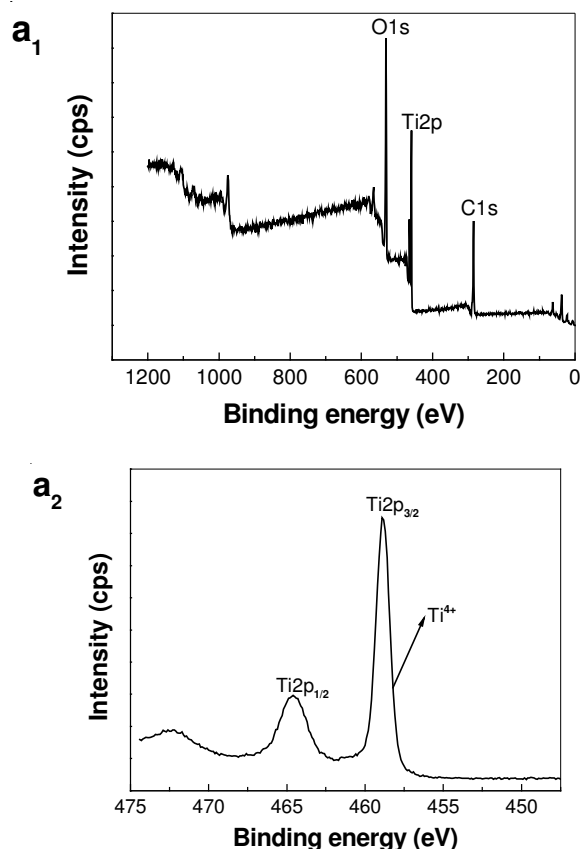
$$\sigma = \sigma_0 \exp \left[-\frac{\Delta E}{KT} \right]$$

where σ_0 is the pre-exponential factor, ΔE is the activation energy for conduction and k is the Boltzmann constant. In this formula, it is assumed that the activation energy (ΔE) is independent of temperature (T). As can be seen, the electrical conductivity of TiO₂ cathode increases with the increasing temperature.

The possible reason may be explained by considering various effects. Firstly, the TiO_{1.95} phase may increase the electron concentration of the system for the electric charge balance, which results in the increase of the electrical conductivity of the obtained TiO₂ cathode. Furthermore, under the low oxygen and high temperature conditions, different oxygen atoms in TiO₂ crystal get different force in which some oxygen atoms with small force obtain enough energy, which leave the equilibrium position to generate oxygen vacancies and an

increase of deviation of stoichiometric ratio. It also increases the electrical conductivity of TiO₂ cathode. From above analysis, the increase of the electrical conductivity is mainly due to the increase in the electron concentration of the system. Therefore, it is believed that TiO_{1.95} generation and oxygen vacancies are fairly effective in achieving high conductivity of TiO₂ cathode. Furtherwork concerning about investigation of detailed mechanism is in progress.

Effect of sintering temperature on oxygen vacancies of TiO₂ cathode: The composition of the titania pellets was measured by XPS. XPS survey spectra of the TiO₂ pellets sintered in argon at 700, 850 and 950 °C are shown in Fig. 6(a₁), (b₁) and (c₁). Ti and O are detected at the surface for all of the samples. Fig. 6(a₂), (b₂) and (c₂) shows Deconvolute XPS Ti2p_{3/2} peak of TiO₂ sintered for the same reaction time of 5 h. If TiO₂ has perfect stoichiometry, then the Ti2p_{3/2} peak should be fitted with only TiO₂ species with a binding energy of about 458.8 eV²⁵⁻²⁷. Fig. 6 (a₂) shows the Ti2p region of the stoichiometric TiO₂ surface. However, curve-fitting of Ti2p_{3/2} of the surface of the TiO₂ pallets sintered in argon at 850 and 950 °C using only TiO₂ species did not give a satisfying result. Some deviations were evident in the range of 456.3-457.5 eV. The lower the number of oxygen atoms bound to Ti in a given species, the lower the binding energy of this species. Therefore, the Ti2p_{3/2} peaks at 456.3 and 457.5 eV *i.e.*, lower than 458.8 eV of TiO₂ species, could best be deconvoluted by invoking the presence of another species. The newly added species is considered to be Ti³⁺, namely TiO_{2-x} as a non-stoichiometric oxide. This result indicates TiO₂ cathode sintered at 850 and 950 °C forms oxygen vacancies, which lead to TiO_{2-x} formation. The defect reaction can be represented as follows²⁸:



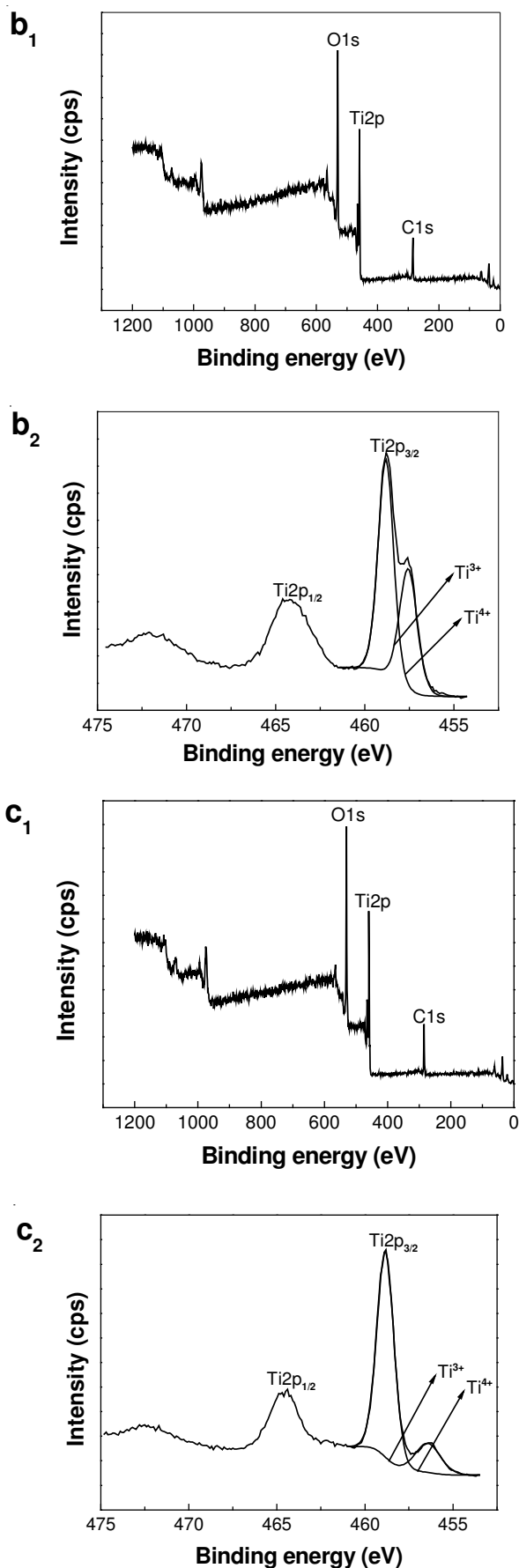


Fig. 6. XPS survey spectra and deconvolute XPS Ti2p_{3/2} peak of TiO₂ sintered for the same reaction time of 5 h at (a) 700 °C (b) 850 °C and (c) 950 °C



The overall reaction formula is:



Table-2 shows the areas and binding energies of the deconvoluted peaks of Ti2p_{3/2} for the TiO₂ samples, along with the TiO_{2-x}/TiO₂ ratios calculated from the areas, which give an indication of the degree of non-stoichiometry. The TiO_{2-x}/TiO₂ ratios of the surfaces of the TiO₂ pallets sintered in argon at 850 and 950 °C were 0.656 and 0.208.

TABLE-1
AREAS AND BINDING ENERGIES OF DECONVOLUTED PEAKS OF Ti2p_{3/2} OF XPS OF TiO₂ AND ARGON ION SPUTTERING SAMPLES AND CALCULATED TiO_{2-x}/TiO₂ AND RELATIVE ATOMIC MOLE RATIOS OF TiO₂

T (°C)	Ti2p _{3/2}				Ti ³⁺ /Ti ⁴⁺
	Ti ⁴⁺ (TiO ₂)		Ti ³⁺ (TiO _{2-x})		
	BE (eV)	Area	BE (eV)	Area	
700	458.8	29010.24	—	—	0
850	458.8	22114.56	457.5	14500.51	0.656
950	458.8	25939.08	456.3	5398.42	0.208

Conclusion

In summary, the influence of sintering temperatures structure and electrical conductivity of TiO₂ was studied. According to the research, we can obtain the following results. First, TiO₂ can be transformed from A→R with the increase of the temperature. And the oxygen vacancies in TiO₂ crystal lead to the formation of low-valence titanium oxide (TiO_{2-x}) at high temperature. Second, the specific surface areas of TiO₂ cathode decrease with the increase of the temperature and adsorption-desorption isotherms and pore size distribution indicate TiO₂ cathode is mesoporous structure. The TiO₂ particle grows larger and tends to be homogenized, the porosity decreases and overall structure tends to be more densification. Finally, the electrical conductivity of TiO₂ increase with the rise of the temperature.

ACKNOWLEDGEMENTS

This work was supported by the Fundamental Research Funds for the Central Universities of China (CDJZR10 22 0003).

REFERENCES

1. M. Sanchez, M.E. Rincon and R.A. Guirado-Lopez, *J. Phys. Chem. C*, **113**, 21635 (2009).
2. U.M. Patil, K.V. Gurav, O.S. Joo and C.D. Lokhande, *J. Alloys Comp.*, **478**, 711 (2009).
3. C. Quinones, J. Ayala and W. Vallejo, *Appl. Surf. Sci.*, **257**, 367 (2010).
4. H. Yoshida, Y. Lu, H. Nakayama and M. Hirohashi, *J. Alloys Comp.*, **475**, 383 (2009).
5. P. Calza, V.A. Sakkas, C. Medana C, M.A. Islam, E. Raso, K. Panagiotou and T. Albanis, *Appl. Catal. B*, **99**, 314 (2010).
6. Y.L. Liao and W.X. Que, *J. Alloys Comp.*, **505**, 243 (2010).

7. P.T. Hsiao, M.D. Lu, T.L. Tung and H.S. Teng, *J. Phys. Chem. C*, **114**, 15625 (2010).
8. S. Ameen, M.S. Akhtar, G.S. Kim, Y.S. Kim, O.B. Yang and H.S. Shin, *J. Alloys Comp.*, **487**, 382 (2009).
9. M.A. Afifi, M.M. Abdel-Aziz, I.S. Yahia, M. Fadel and L.A. Wahab, *J. Alloys Comp.*, **455**, 92 (2008).
10. F. Yakuphanoglu, M. Okutan and K. Korkmaz, *J. Alloys Comp.*, **450**, 39 (2008).
11. W.Y. Wang, D.F. Zhang, T. Xu, X.F. Li, T. Zhou and X.L. Chen, *J. Alloys Comp.*, **335**, 210 (2002).
12. F.M. Meng, *Mater. Sci. Eng. B*, **117**, 77 (2005).
13. C. Wu, Y. Yue and X. Deng, *Catal. Today*, **93/95**, 863 (2004).
14. R.M. Mohamed and I.A. Mkhaliid, *J. Alloys Comp.*, **501**, 143 (2010).
15. V. Belessi, G. Romanos, N. Boukos, D. Lambropoulou and C. Trapalis, *J. Hazard. Mater.*, **170**, 836 (2009).
16. K.V. Baiju, P. Periyat, P. Shajesh, W. Wunderlich, K.A. Manjumol, V.S. Smitha, K.B. Jaimy and K.G.K. Warriar, *J. Alloys Comp.*, **505**, 194 (2010).
17. I.M. Hung, Y. Wang, C.F. Huang, Y.S. Fan, Y.J. Han and H.W. Peng, *J. Eur. Ceram. Soc.*, **30**, 2065 (2010).
18. X.M. Yan, P. Mei, J.H. Lei, Y.Z. Mi, L. Xiong and L.P. Guo, *J. Mol. Catal. A: Chem.*, **304**, 52 (2009).
19. D.S. Kim, S.J. Han and S.Y. Kwak, *J. Colloid Interf. Sci.*, **316**, 85 (2007).
20. M.M. Viana, V.F. Soares and N.D.S. Mohallem, *Ceram. Int.*, **36**, 2047 (2010).
21. R.C. da Silva, E. Alves and M.M. Cruz, *Nucl. Instr. Meth. Phys. Res. B*, **191**, 158 (2002).
22. P.S. Patil, S.H. Mujawar, A.I. Inamdar, P.S. Shinde, H.P. Deshmukh and S.B. Sadale, *Appl. Surf. Sci.*, **252**, 1643 (2005).
23. K. Karthik, S.K. Pandian and N.V. Jaya, *Appl. Surf. Sci.*, **256**, 6829 (2010).
24. A. Holt and P. Kofstad, *Solid State Ionics*, **117**, 21 (1999).
25. K. Bubacz, J. Choina and J.D. Dolat, *Mater. Res. Bull.*, **45**, 1085 (2010).
26. J.A. Zou, J.C. Gao and F.Y. Xie, *J. Alloys Comp.*, **497**, 420 (2010).
27. G. Li, F. Liu and Z. Zhang, *J. Alloys Comp.*, **493**, L1 (2010).
28. B.Y. Li, D.X. Zhou, S.L. Jiang, Z.W. Lv and S.P. Gong, *Piezoelectrics Acoustooptics*, **23**, 473 (2001).